CHAPTER – 3

Experimental Work

This chapter comprises all the details of the experimental work. Characterization includes microstructure, mechanical properties, and tribological properties of prepared samples.

3.1 Flow of the Experimental Work

Experimental work was divided into five phases in this research. The plan of experimental work is described in below Figure 3.1.

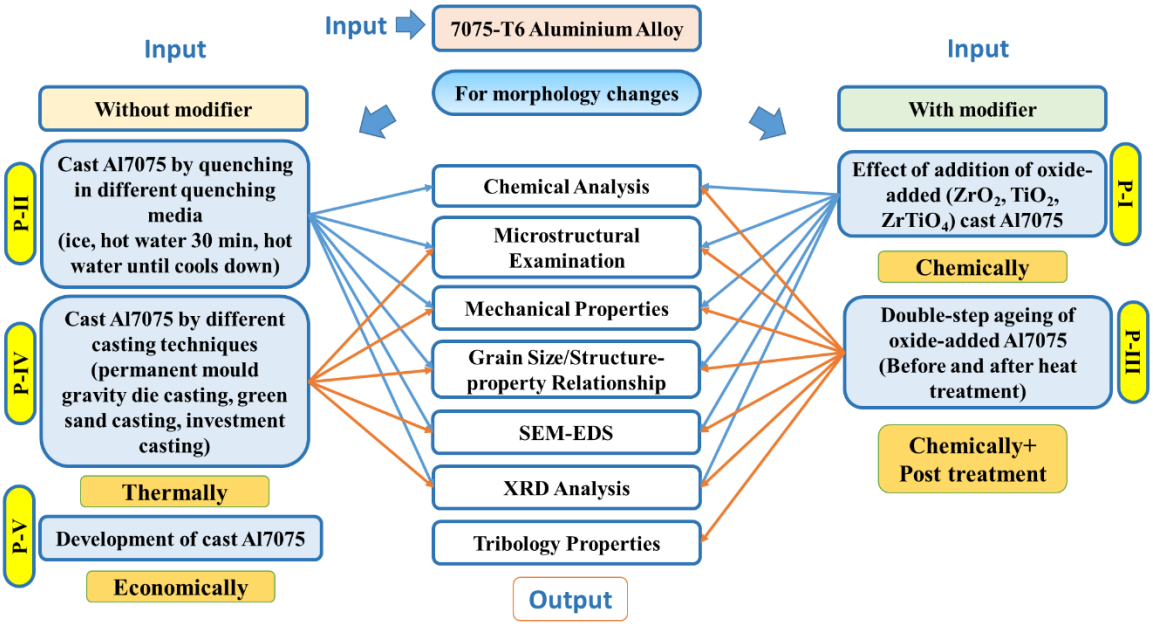

Figure 3.1 Plan of experimental work: Phase I & II with modifiers addition (right side), and Phase III, IV, and V without modifiers (left side).

3.2 Raw materials and their characterization

Al 7075-T6 in the wrought condition is procured for the present experiment. The plate of 45 mm is cut into a small block of approximately 500 grams and then used for experimental work, as shown in Figure 3.2.

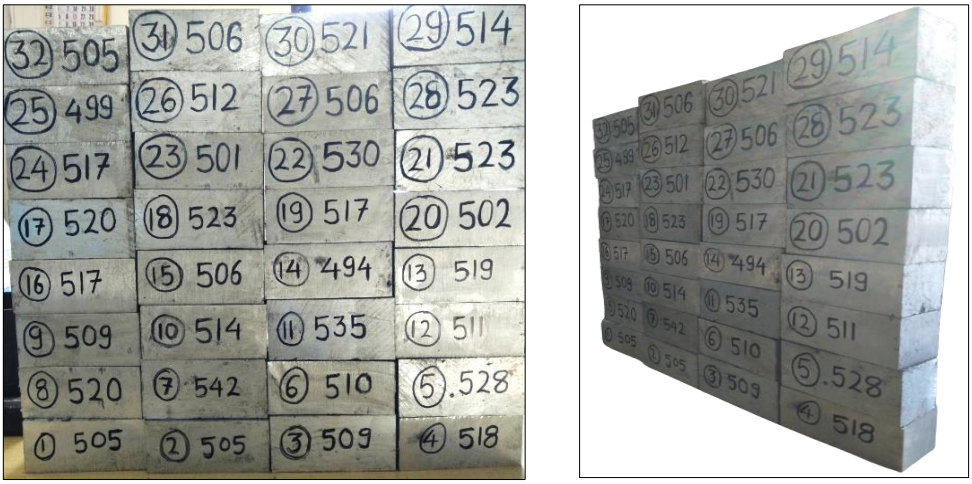

Figure 3.2 Raw material for the experiment (Al7075-T6).

The as-received material is analysed for bulk chemical composition by optical emission spectrometry (OES). The laboratory grade ZrO_2, TiO_2 and $ZrTiO_4$ are procured as modifiers to add into Al 7075 and characterize their purity, size and shape by SEM-EDS. Hexachloroethane tablet is used for degassing the melt. The aluminium rod is used to rotate the liquid melt for homogeneous mixing.

3.3 Experimental Set-up

The experimental set-up for melting of Al 7075 is shown in Figure. A crucible-type furnace with kanthal wire winding, RTD sensor, and controller is used for resistance heating. A metallic die is used to pour the liquid melt, and the dimensions are also shown in Figure 3.3.

Figure 3.3 Experimental set-up for melting Al7075 (left), and metallic die with dimensions to pour liquid melt.

The resistance heating furnace temperature is set at 730 °C. The schematic of the metallic die is shown in Figure 3.4. For every heat, a quantity of 1 kg of Al 7075 is utilized. The furnace top lid is closed during melting to avoid atmospheric interaction of liquid melt.

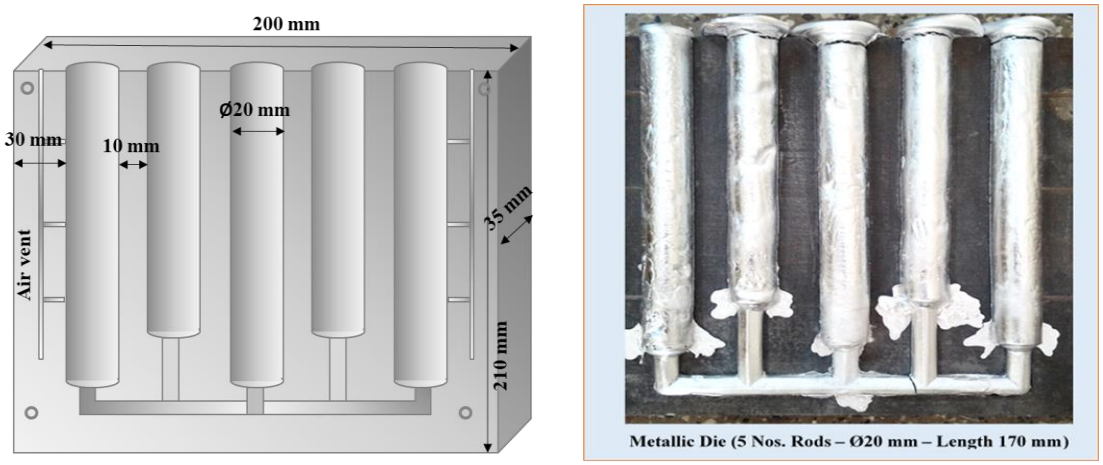

Figure 3.4 Schematic of metallic die (right), and solidified casting in the die (left).

3.4 Experimental procedure

The experiments are divided into five phases to characterize the Al 7075 by using modifiers and heat treatment. Five phases are planned as below, out of that, Phase I and Phase II with modifiers addition, and Phase III, and Phase IV without modifier addition.

Phase I	Effect of the oxide addition into cast Al 7075.
Phase II	Effect of quenching medium on cast Al 7075.
Phase III	Effect of double-step ageing on the oxide-added cast Al 7075.
Phase IV	Effect of different casting techniques of cast Al 7075.
Phase V	Development of cast Al 7075 by alloy addition.

The process flow of the above phases is outlined below.

3.4.1 Effect of the oxide addition into cast Al7075.

The process flow of the melting, degassing, oxide addition, pouring, and sampling is done for the characterization, and is shown in Figure 3.5. The individual 2.5 wt.% oxides are added to the melt based on the literature.

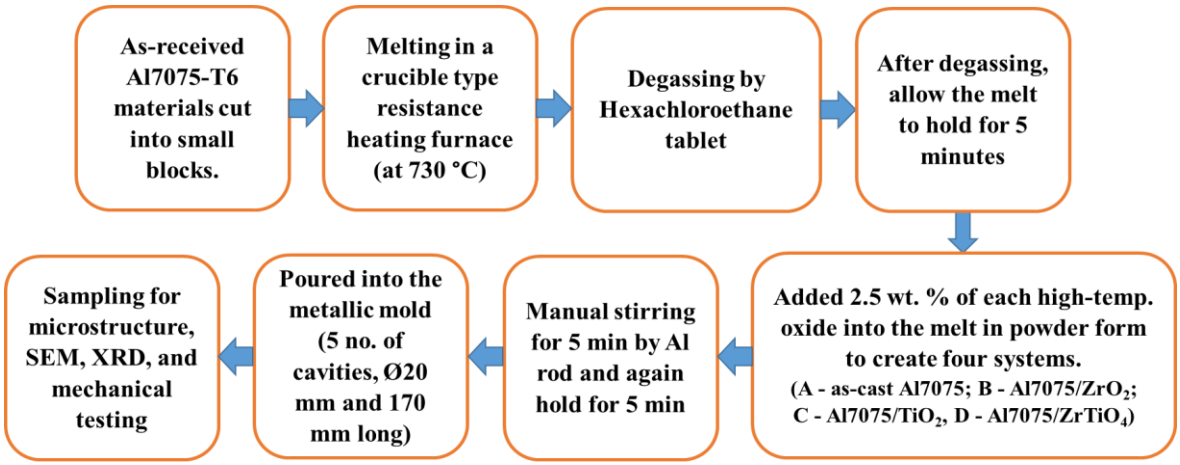

Figure 3.5 Process flow diagram for Phase I.

3.4.2 Effect of quenching medium on cast Al 7075.

The process flow of the cast Al 7075 with different quenching conditions is shown in Figure 3.6.

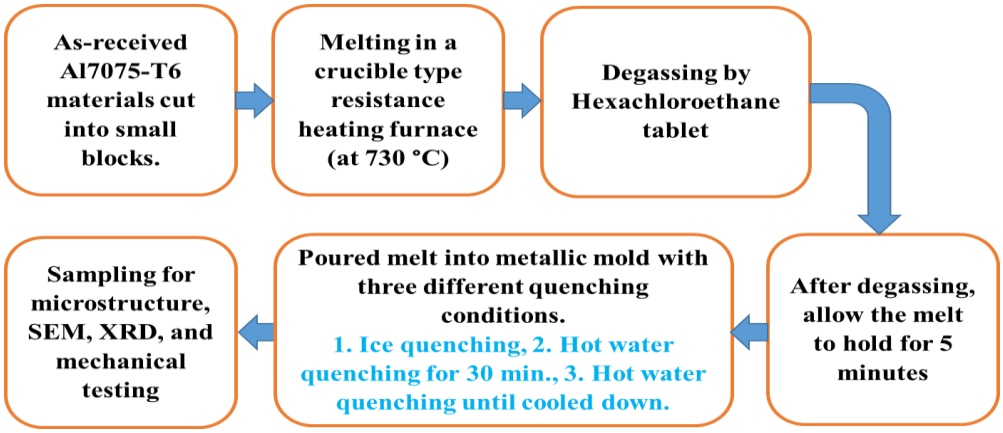

Figure 3.6 Process flow for Phase II.

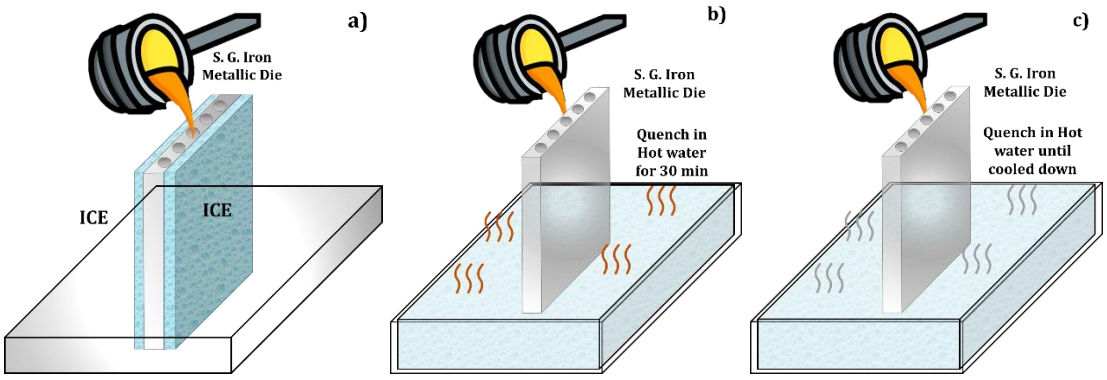

Figure 3.7 Schematic diagram of quenching of cast Al 7075 during solidification with different

quenching conditions: a) ice, b) hot water for 30 min, and c) hot water until cooled down.

The schematic illustration of the quenching conditions is shown in Figure 3.7.

3.4.3 Effect of double-step ageing on the oxide-added cast Al 7075.

The process flow for double-step ageing is shown in Figure 3.8.

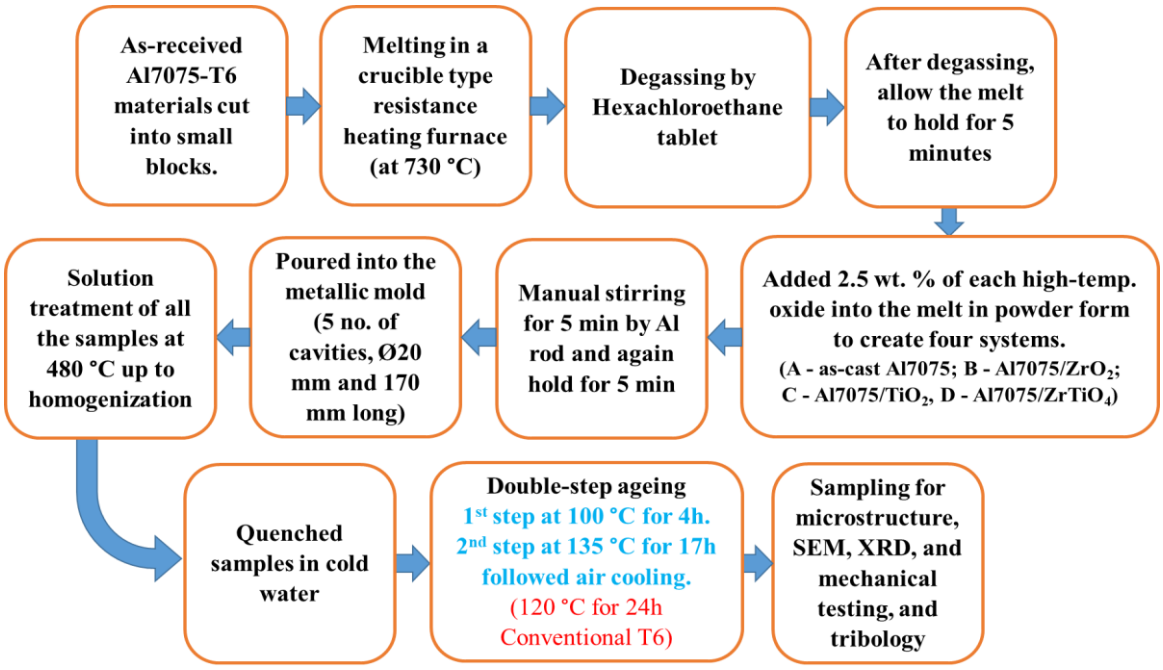

Figure 3.8 Process flow for Phase III.

The heat treatment cycle for treating oxide added Al7075 is shown in Figure 3.9.

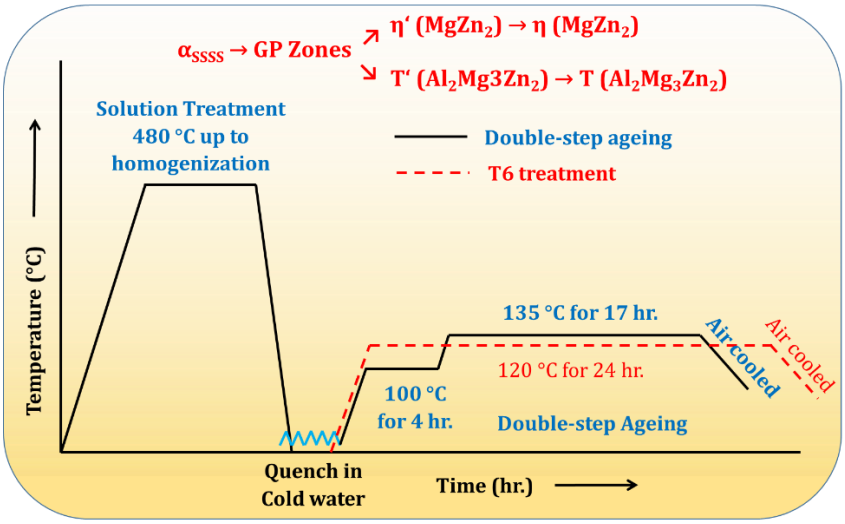

Figure 3.9 Double-step ageing cycle for oxide-added cast Al 7075.

3.4.4 Effect of different casting techniques of Al 7075

Different casting techniques like gravity die casting, green sand moulding, and investment casting are employed to produce the cast Al 7075. The described processes differ by their mould characteristics and their ultimate effect on the microstructure and mechanical properties. The difference in the heat dissipation of the moulds creates an effective thermal gradient, which causes a change in the microstructure and mechanical properties. The process flow diagram is shown in Figure 3.10.

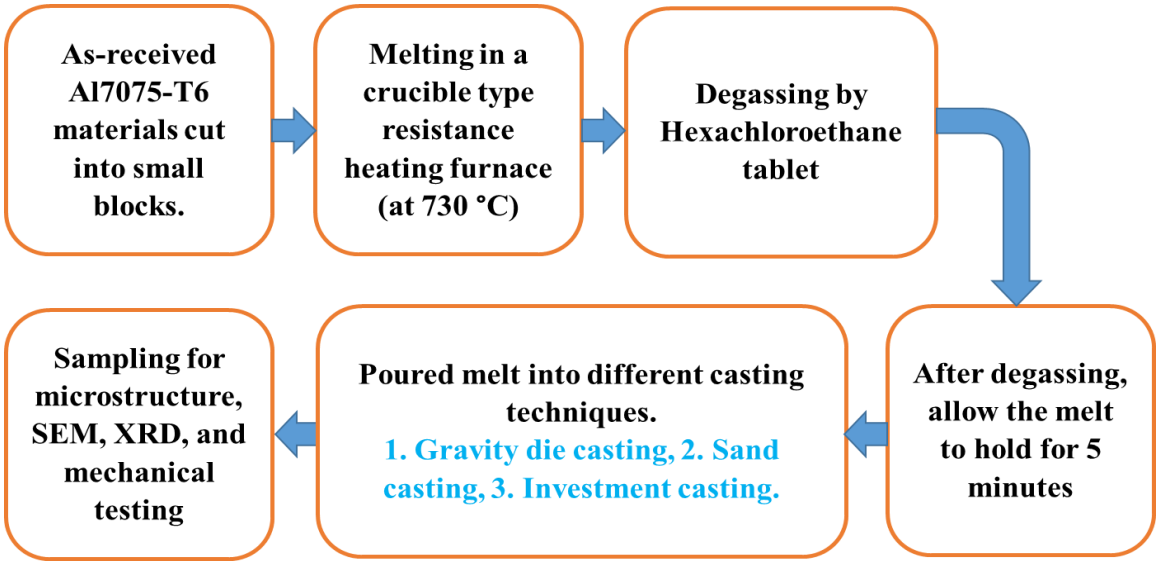

Figure 3.10 Process flow of Phase IV.

The schematic illustration of different casting techniques is shown in Figure 3.11.

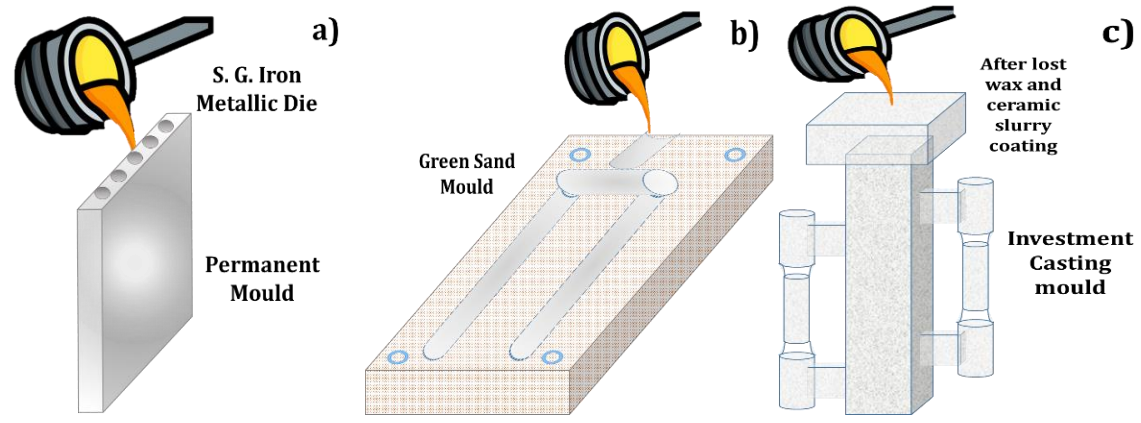

Figure 3.11 Schematic illustration of casting techniques: a) gravity die casting, b) sand casting and c) investment casting.

3.4.5 Development of cast Al 7075 by alloy addition.

For the economic development of cast Al 7075, different scraps are used to make an alloy of Al 7075. The recycling of the materials reduces the cost of the alloy. The process adopted to develop it is described in Figure 3.12.

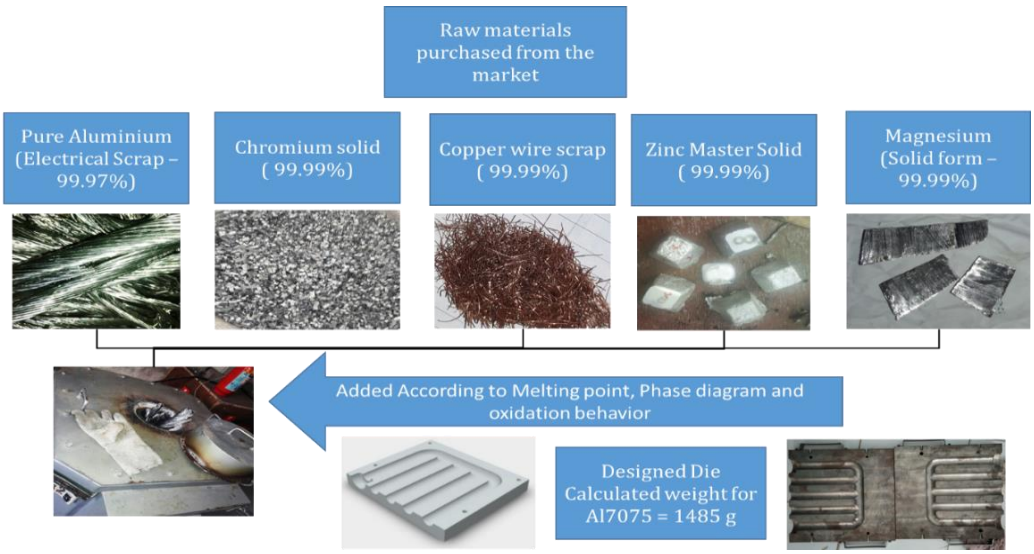

Figure 3.12 Process adopted to develop cast Al 7075.

3.5 Metallography procedure, and microscopy

Metallographic sampling is done by using a lathe machine and cutting it to the needed size and shape. The samples are prepared by standard metallography procedure, i.e. cutting, grinding, dry & wet polishing, fine polishing, and etching. The polished samples are etched with diluted 0.5 percent HF solution. The microstructural examination is done by using an inverted Olympus GX41 metallurgical microscope, as shown in Figure 3.13.

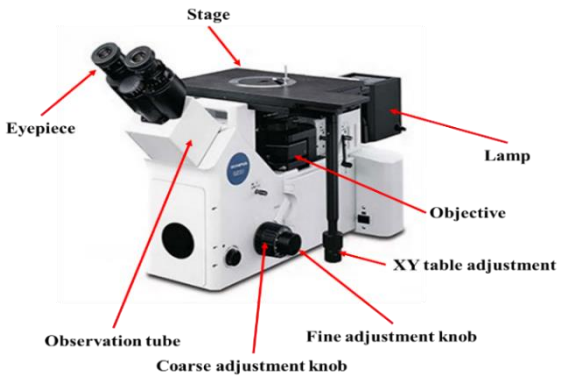

Figure 3.13 Olympus GX41 metallurgical microscope.

The grain size measurement is made using ImageJ software. Analytical scanning electron microscopy is done for the samples by JEOL JSM 7900F and JEOL JSM 5610LV. Scanning electron microscopy photographs are captured with these systems. The quantitative and qualitative analysis of samples is done by energy dispersive spectroscopy with Oxford Ultimax. JEOL JSM 7900F facility is available at CIF-IIT-Gandhinagar, as shown in Figure 3.14, and JEOL JSM 5610LV at MSU, Baroda.

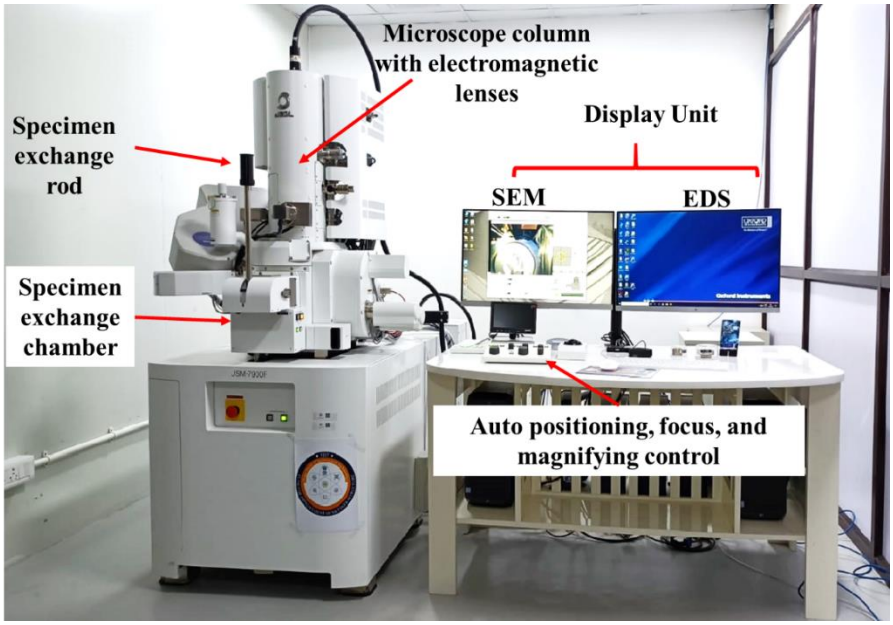

Figure 3.14 Analytical scanning electron microscope (JEOL JSM 9600F).

3.6 XRD analysis

Figure 3.15 XRD analysis Malvern PANanalytical X'Pert Pro machine.

The XRD analysis is used to confirm the intermediate phase formation in the samples. The Ø 15-20 mm, 2 mm thick fine polished sample was prepared before the testing. Malvern PANanalytical X'Pert Pro machine is used to test all the samples with Cu Kα radiation (λ = 1.54 Å), 40 mA & 45 kV generator settings, and scan ranges of 2θ between 10° to 90 °. The machine is shown in Figure 3.15. The analysis of the XRD patterns is evaluated using the X'Pert Highscore plus software.

3.7 Mechanical testing

The hardness testing and tensile testing are carried out to get the mechanical properties.

3.7.1 Hardness testing

The Brinell hardness testing was carried out on each sample at six different locations, and an average was reported. The load is 62.5 kg, and the 2.5 mm diameter tungsten indentor is used. Omnitech MVH-S Auto micro-hardness tester, having a load range of 1g to 2000g, is used to measure the micro-hardness at a 500g load for 10s dwell time.

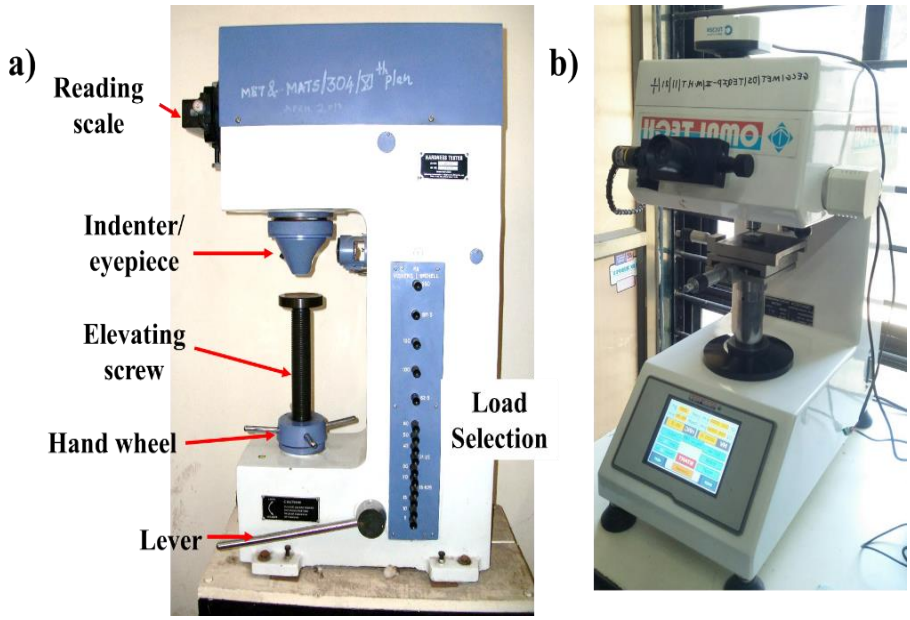

Figure 3.16 (a) Brinell hardness tester, (b) micro-hardness tester (Omnitech MVH-S Auto).

The depth of an indentation in microns and micro-hardness was reported in $HV_{0.5}$. The schematic diagram of a Brinell hardness tester is illustrated in Figure 3.16 (a), with a micro-hardness tester represented in Figure 3.16 (b).

3.7.2 Tensile testing

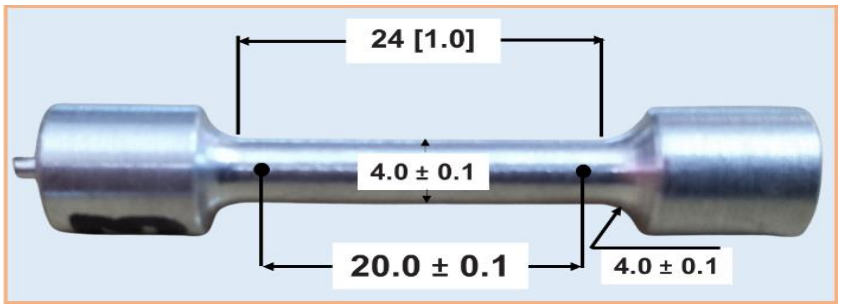

Figure 3.17 Tensile testing specimen as per ASTM E8M.

The ultimate tensile strength and percentage elongation are measured based on an average of three readings. The dimensions of the tensile testing specimen prepared according to ASTM E8M with a gauge length five times the diameter are shown in Figure 3.17.

The tabletop Monsanto Tensometer 20 is used to test the all samples. The transverse crosshead moves at 0.5 mm/min, and the load is 20 KN. Percentage reduction and elongation are checked using gauges, as shown in Figure 3.18.

Figure 3.18 Table top tensometer for tensile testing ("MONSANTO" make Tensometer20) with specimen holder for round samples and %RA & %EL. Gauges.

3.8 Tribology

The tribology analysis is conducted on the samples before and after the heat treatment. The

wear performance of the developed sample was assessed through a wear test with the pin-on-disc wear testing machine (DUCOM make, model: TR-20E-PHM-300), based on the rotational speed, applied load, and rpm, set-up is as shown in Figure 3.19.

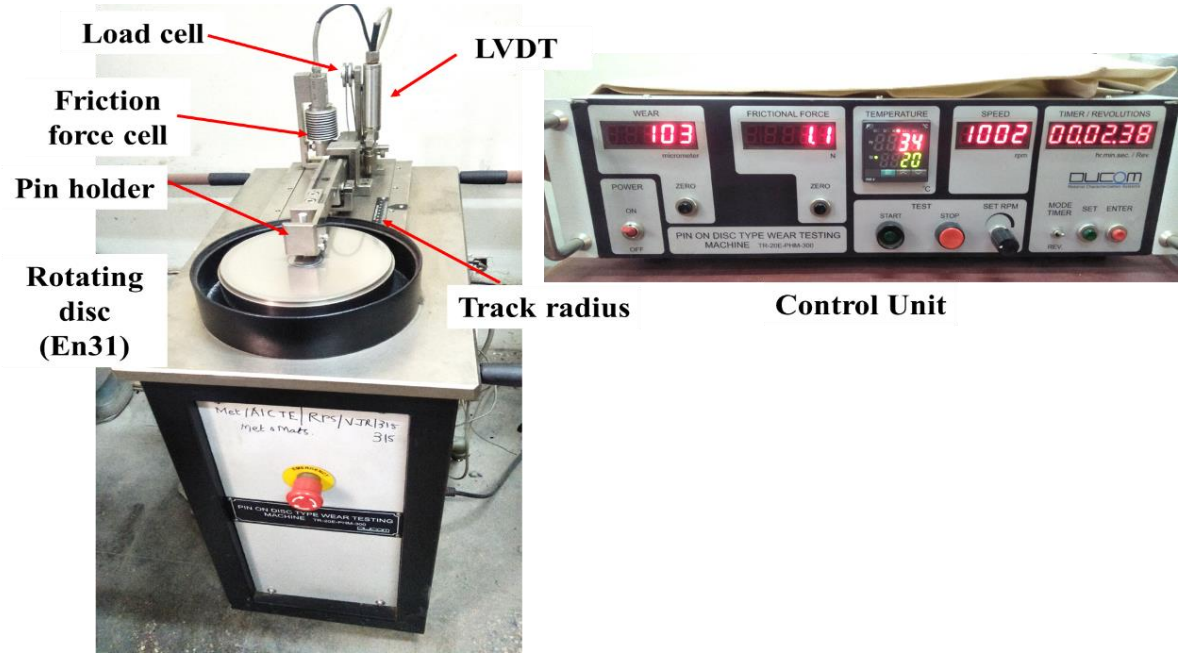

Figure 3.19 Pin-on-disc wear testing machine DUCOM make model: TR-20E-PHM-300.

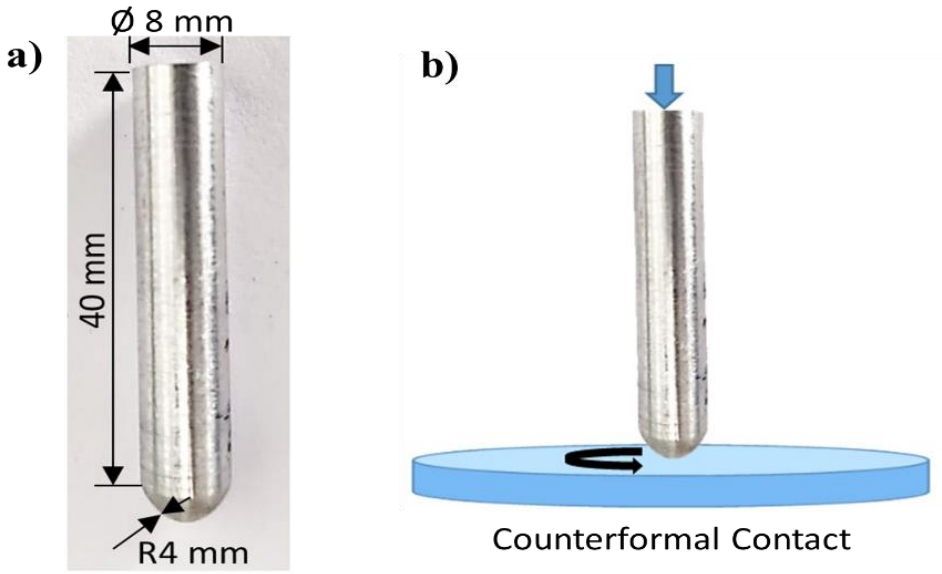

Figure 3.20 (a) Pin-on-disc wear testing specimen as per ASTM G99, b) counterformal contact of sliding wear.

The test conditions and specimen material are given in Table 3.1.

Table 3.1 Operating parameters for tribology of oxide-added samples at various applied loads and rotational speed.

Test Condition		Specimen Material
Normal load in N	10, 20, 30, 50 (For all specimens)	**Stationary pin: Ø 8 mm** **(Before and after heat treatment)** 1. Al 7075 as-cast 2. 2.5 wt.% ZrO_2 added Al 7075 3. 2.5 wt.% TiO_2 added Al 7075 4. 2.5 wt.% $ZrTiO_4$ added Al 7075 **Rotating Disc:** EN31 hardened to 62 HRC **Density of Al 7075 pin:** 2.81 g/cc
The rotational speed of the disc at rpm	500, 700, 100 (For all specimens)	
Time in sec	1274@500 rpm 910@700 rpm 634@100 rpm	
Sliding distance in meter (Sliding distance =(circumference*rpm*time)	1000 m (fixed)	
Wear track dia. in mm	30 mm	

The specimen was prepared under ASTM G99, displayed in Figure 3.20 (a). The specimen had a height of 40 mm and a diameter of 8 mm, with a dome-shaped contact having a 4 mm radius of curvature. The specimen was checked against the rotating disc using a counterformal contact, as shown in Figure 3.20 (b). The fixed 1000 m of sliding distance was maintained for various rotations per minute of 500, 700, and 1000 as well as average load of 10, 20, 30, and 50 N, to determine the wear properties at room temperature. The precision weighing scale of 0.0001 mg was used to weigh samples before and after each test.

3.9 Structure-property relationship

The structure-property relationship is established using the Hall-Petch equation. The plot of micro-hardness versus grain diameter establishes the trend of the grain boundary hardening as the grain diameter reduces. ImageJ software is used to determine average grain size and area.

.